

# Mathematical Connections through Eigenvalue Spacings

Kelly Romer

May 1, 2022

## 1 Introduction

In “Finite Quantum Chaos”, mathematician Audrey Terras introduces a concept called the Tree of Quantum Chaos[3]. Terras, alongside other mathematicians, has used this tree as a motivation for research. The Tree of Quantum Chaos (Figure 1) depicts the relationship between 6 areas of mathematics. The branches of the tree are quantum physics, geometry of number theory, and graph theory. The roots are the Gutzwiller trace formula, the Selberg trace formula, and the Ihara zeta function[2]. What the Tree of Quantum Chaos suggests is that there are fundamental structures that the branches and roots of the tree may share with each other. In other words, patterns found in one branch or root may lead to discoveries about another. Ultimately, the Tree of Quantum Chaos visually depicts the motivation to discover the “stochastic laws governing sequences having very different origins”[2]. Each branch generates a sequence of numbers: eigenvalues, prime numbers, etc. The hope is that there are some similarities between these sequences. Terras in particular endeavors to discover connections between the branches and roots of the tree. In this paper, this motivation is narrowed down to seeking connections between two branches: quantum physics and graph theory.

### 1.1 Quantum Physics and Graph Theory

In quantum physics, energy levels  $E$  of a physical system are the eigenvalues of the Schrödinger equation,  $H\phi = E\phi$ . Because it is often impossible to know all energy levels, mathematicians investigate the statistical theory of the energy levels to learn about their behavior[2]. In linear algebra, the Schrödinger operator is on an infinite dimensional vector space. Graph theory allows this operator to be replaced with a finite analogue: the adjacency matrix (operator) of a graph[2]. Mathematician M.E. Starzak summarizes this concept well: “think of a graph as a system of masses connected by rubber bands. This is a reasonable model for a molecule”[3]. In this paper, the eigenvalues of several matrices will be studied in an endeavor to seek knowledge regarding energy



Figure 1: Tree of Quantum Chaos

levels in quantum physics. In particular, modeling the eigenvalues as spectra allows for comparisons to be made to spectra of energy levels.

## 1.2 Contents

This paper is divided into 4 main sections: Methodology, Matrix Generation Cases, and Results and Observations, and Future Work. In Section 2, we describe our methodology. In particular, the process of generating eigenvalues is detailed, with use of an example. Additionally, the various statistical equations used to study the eigenvalues are explained. In Section 3, Eigenvalue Generation Cases, the mathematical structure of each source of eigenvalues is provided, including both necessary mathematical background knowledge and reasoning as to why these sources were chosen. Next, in Section 4, all note-worthy results and observations regarding these eigenvalues and their spectra will be explained in detail. Finally, the paper will conclude with ideas for future work in Section 5.

## 2 Methodology

Eigenvalues are generated from matrices from a variety of sources, which will be highlighted in a Section 3. The focus of this section is to explain the pipeline from eigenvalue generation to observation.

### 2.1 $n$ -gon Example of Methodology

In order to understand the methodology for generating and studying eigenvalues, we begin with an example. In this example, the eigenvalues stem from the adjacency matrix of an  $n$ -gon<sup>1</sup>. The first step in this process is generating the  $n$ -gon and creating the adjacency matrix from the  $n$ -gon. The  $n$ -gon is a graph of  $n$  vertices, where each vertex is connected by an edge to 2 other vertices, forming a polygon of  $n$  sides and edges. An adjacency matrix is an  $n \times n$  square matrix where each row  $1 \dots n$  and each column  $1 \dots n$  represents a vertex of a graph. For each entry  $a_{i,j}$ , if an edge exists between vertex  $i$  and vertex  $j$ , set  $a_{i,j} = 1$ . If no edge exists between the two vertices, set  $a_{i,j} = 0$ . Next, the eigenvalues from the adjacency matrix are calculated and sorted from least to greatest,  $\lambda_1 \leq \lambda_2 \leq \dots \leq \lambda_n$ . Assume that there are at least 2 unique eigenvalues.  $\lambda_1 \dots \lambda_n$  are then normalized between 0 and 1 using the **normalization equation**

$$\forall i = 1, 2, \dots, n, \quad \hat{\lambda}_i = \frac{\lambda_i - \lambda_1}{\lambda_n - \lambda_1} \quad (1)$$

This makes it easier to compare different sets of eigenvalues with the focus of identifying patterns in eigenvalue spreads. Once these eigenvalues are normalized, they are plotted on a histogram and the statistical equations in Section 2.3 are used to gain a better understanding of eigenvalue skew and concentration. Now, they may be compared against other sets of eigenvalues derived from different matrices but prepared in the same manner.

### 2.2 Summary of Steps

In general, the first step in the methodology process is to create a matrix to derive eigenvalues from. In the case of the  $n$ -gon, it is derived from a graph which must be created. In other cases, a matrix is populated using a probability distribution, which will be elaborated on in Section 3. Next, we calculate the eigenvalues from the given matrix. Then, the eigenvalues are scaled between 0 and 1 using the normalization equation (1). Finally, the eigenvalues are plotted on a histogram and calculations are made using each equation in Section 2.3. Now, the eigenvalues are ready to be observed - both visually, through the histogram, and statistically, through the equations. Eigenvalues derived from each source will be compared with each other.

---

<sup>1</sup>Each  $n$ -gon is a Cayley graph generated from a cyclic permutation group.

## 2.3 Statistical Equations

**Mean:** The mean indicates where the scaled eigenvalues typically fall in the range  $[0, 1]$ . Thus, it is an indicator of the left/right skew of the eigenvalues.

$$\bar{\lambda} = \frac{1}{n} \left( \sum_{i=1}^n \lambda_i \right) \quad (2)$$

**Standard Deviation:** The standard deviation indicates the distance of eigenvalues from the mean. For instance, if the standard deviation is high, it indicates that eigenvalues generally occur far from the mean.

$$\sigma = \sqrt{\frac{\sum_{i=1}^{n-1} (\lambda_i - \bar{\lambda})^2}{n}} \quad (3)$$

**Centralization:** In contrast to standard deviation, centralization detects the average distance from the center of the spread, rather than distance from the mean.

$$\tilde{\sigma} = \sqrt{\frac{\sum_{i=1}^{n-1} (\lambda_i - \frac{1}{2})^2}{n}} \quad (4)$$

**Successive Spacings:** The equation for successive spacings detects large spacings between successive eigenvalues. The equation is similar to that of  $\sigma$  and  $\tilde{\sigma}$ , but rather than finding the average distance from the mean or  $\frac{1}{2}$ , it calculates the distance between each pair of successive eigenvalues and calculates the average of that distance.

$$\xi = \sqrt{\frac{\sum_{i=1}^{n-1} (\lambda_i - \lambda_{i+1})^2}{n}} \quad (5)$$

**All Spacings:** This equation detects large spacings between all pairs of eigenvalues. The numerator takes the positive distance between all possible combinations of eigenvalue pairs. The denominator is derived as follows: if the distance between an eigenvalue and itself is not considered, then there are  $n \cdot (n - 1)$  possible pairs of eigenvalues. Furthermore, since pairs of eigenvalues should not be counted twice depending on the order, divide  $n \cdot (n - 1)$  by two: this equates to  $\binom{n}{2}$ .

$$\tilde{\xi} = \sqrt{\frac{\sum_{1 \leq i < j \leq n} (\lambda_i - \lambda_j)^2}{\binom{n}{2}}} \quad (6)$$

### 3 Eigenvalue Generation Cases

#### 3.1 Adjacency Matrices of n-gons (Case n-g)

In the Section 2, an example execution of this case is demonstrated; an adjacency matrix is derived from the graph of an  $n$ -gon. These graphs inherently contain no loops, ensuring a diagonal populated with 0's. Furthermore, the adjacency matrices that these graphs yield are inherently symmetric because the graphs of  $n$ -gons are undirected.

#### 3.2 Random 50x50 Adjacency Matrices with 0 Diagonal (Case RA)

In the case of random  $50 \times 50$  adjacency matrices with zero diagonal, each entry in the matrix is populated with either zero or one, chosen randomly. The objective of this is to obtain a matrix that mimics an adjacency matrix; a value of '1' at a given entry  $a_{i,j}$  would represent a connection by an edge between two vertices  $i$  and  $j$ . A value of '0' at the same spot would imply otherwise. Whether a given entry is a zero or a one is determined by *binomial distribution*, a probability distribution in which the outcome is either 1, representing a success, or 0, representing a failure. It is important to note that each entry is chosen independently of the others. The probability of success, or the number '1' being selected, is equal to the success rate  $p$ . The impact of this on the distributions of eigenvalues is significant and will be observed in Section 4. The matrix is created as follows: if  $i < j$ , then  $a_{i,j}$  is chosen randomly with binomial distribution. When  $i = j$ ,  $a_{i,j}$  is set to 0 to simulate an adjacency matrix from a graph with no loops. When  $i > j$ , set  $a_{i,j} = a_{j,i}$  to create a symmetric matrix. This simulates the adjacency matrix of an undirected graph, and ensures only real eigenvalues are generated.

#### 3.3 200 Real 50x50 Symmetric Matrices

For this case, 200 individual  $50 \times 50$  symmetric matrices are created as follows. First, a  $50 \times 50$  matrix is created and each entry  $a_{i,j}$  such that  $i < j$  is populated with a number between 0 and 1, chosen independently with either *standard normal distribution* or *uniform distribution*.

##### Standard Normal Distribution (Case RSN)

On a Standard Normal Distribution curve,  $\mu = 0$  and  $\sigma = 1$ . Values are symmetrically distributed around the mean, and the area under the curve (Figure 2) is equal to 1. When using standard normal distribution as a mechanism for populating matrices, the entries will be near 0 with the highest likelihood, and the likelihood of a value being chosen decreases with its distance from 0.

##### Uniform Distribution (Case RSU)

Uniform distribution chooses any number on the continuous spectrum with ran-

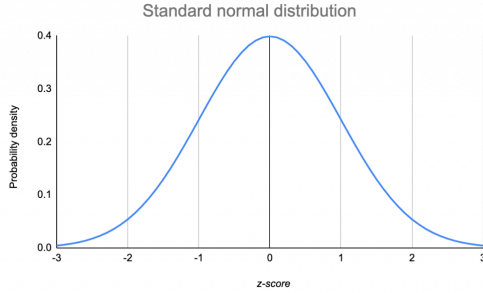


Figure 2: Standard Normal Distribution Curve, from [1]

domness. The specified range chosen in this project for selecting values to populate the  $50 \times 50$  matrices is  $[0, 1]$ . While still symmetric around the mean, unlike standard normal distribution, it is important to note that all values between 0 and 1 are equally likely to be chosen.

Next, set every  $a_{i,i} = 0$  to ensure a graph with no loops. Then, for all entries  $a_{i,j}$  such that  $i > j$ , set  $a_{i,j} = a_{j,i}$  to create a symmetric matrix. It is important to note that these matrices, unlike adjacency matrices, can have entries of any number *within*  $[0, 1]$ , rather than *either* 0 *or* 1. The impact of this difference will be observed in Section 4. Lastly, each set of eigenvalues gained from these 200 matrices are averaged together. Rather than studying the individual eigenvalues of each of these matrices, the focus is on the overall behavior they collectively depict.

### 3.4 Uniform Distribution (Case U)

In this case,  $n$  numbers between 0 and 1 are generated, each using uniform distribution. In contrast to previous cases, Uniform Distribution itself generates a spectrum of numbers. This spectrum serves as a base for comparison against spectra of eigenvalues.

### 3.5 Poisson Spectrum (Case P)

For this case,  $n$  numbers are generated using the Poisson distribution. In the same manner as the uniform distribution case, the Poisson distribution directly provides a spectrum of numbers. According to the Poisson distribution,  $\forall x \in \mathbb{N}$ , the probability of selecting  $x$  is  $\frac{\lambda^x}{x!}e^{-\lambda}$ , where  $\lambda$  indicates the expected rate of occurrences. Most numbers get clumped around the size of  $\lambda$ , which is set to 500 in this case.

## 4 Results and Observations

Table 4 contains a summary of statistical analysis for each eigenvalue generation case.

Table 1: Statistics for Case Samples

	50-G	RA**	RSN	RSU	U*	P*
$\lambda$	0.5	0.19899	0.48976	0.15258	0.49964	0.48748
$\sigma$	0.35355	0.15547	0.23114	0.13255	0.28893	0.15910
$\tilde{\sigma}$	0.35355	0.33879	0.23136	0.37184	0.28893	0.15959
$\xi$	0.28798	0.00887	0.12452	0.16630	0.40949	0.21935
$\tilde{\xi}$	0.49033	0.14885	0.32682	0.18708	0.40861	0.22488

\* 200 iterations, averaged

\*\* Success rate  $p = 0.5$

### 4.1 Symmetry of Eigenvalues of $n$ -gons

Eigenvalues of ‘special’ matrices, such as adjacency matrices of  $n$ -gons, have unique properties that eigenvalues from random matrices do not. Terras notes that symmetry groups have a large effect on energy levels[2]. The  $n$ -gons are polygons with rotational symmetry of  $\frac{360}{n}$  degrees. Similarly, the spectra of their eigenvalues is symmetric around the mean, which is always  $\bar{\lambda} = \frac{1}{2}$ . This can be seen in Figure 3, which is a histogram of normalized eigenvalues from the adjacency matrix of a 20-gon. Another interesting observation regarding the

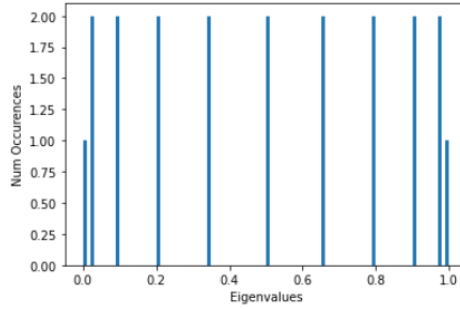


Figure 3: Histogram of normalized eigenvalues from adj. matrix of 20-gon

eigenvalues of the adjacency matrices of  $n$ -gons is that the gaps between them decrease as they move further away from the center. This can be seen visually through the histogram of eigenvalues from a 20-gon (Figure 3) and the histogram of eigenvalues from a 100-gon (Figure 4). Table 2 shows that the average spacing

between subsequent eigenvalues,  $\xi$ , decreases while the centralization  $\tilde{\sigma}$  remains constant. A consistent  $\tilde{\sigma}$  indicates that the average distance of eigenvalues from the center remains consistent as the number of eigenvalues increases. A decreasing  $\xi$  tells us that as the amount of eigenvalues increases, the distance between them decreases. In other words, while these histograms become more saturated, the distribution of eigenvalues throughout them remains consistent.

Table 2:  $n$  vs.  $\tilde{\sigma}$ , and  $\xi$

$n$	$\tilde{\sigma}$	$\xi$
20	0.35355	0.42064
50	0.35355	0.28798
100	0.35355	0.25772

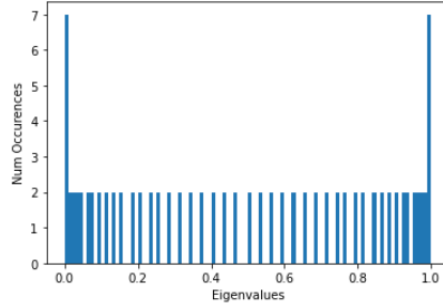


Figure 4: Histogram of normalized eigenvalues from adj. matrix of 100-gon

Random adjacency matrices, in contrast do not yield eigenvalues that demonstrate special properties. For example, reference Figures 9 and 10 in Section 4.3. There is a clear lack of symmetry. Table 3 demonstrates that  $\bar{\lambda}$  is always below  $\frac{1}{2}$  for random adjacency matrices, and that eigenvalues tend to cluster near this lower average.

## 4.2 The Wigner Semi-Circle

When looking at eigenvalues of a  $50 \times 50$  real, symmetric matrix whose entries were populated independently using standard normal distribution (Figure 5), there is no particularly dominant pattern. However, when the eigenvalues of several of these matrices are analyzed on the same histogram, a semi-circle becomes distinguishable.

In the 1950's, physicist and mathematician Eugene Wigner noted that energy levels could be modeled with large real symmetric matrices whose entries



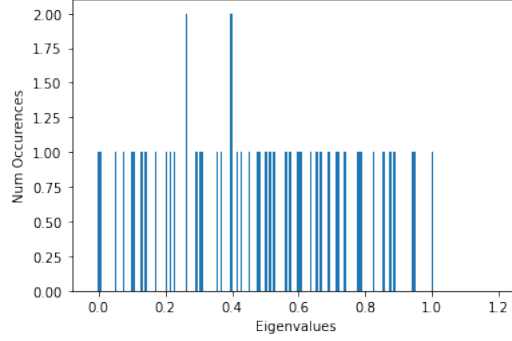


Figure 5: Histogram of eigenvalues from 1 RSN

are chosen with normal distribution[2]. Furthermore, Wigner observed that the histogram of the eigenvalues from such a matrix resembles a semi-circle. This phenomenon is the *Wigner Semi-Circle*. The Wigner Semi-Circle can be seen in the histogram of eigenvalues from 200 real, symmetric  $50 \times 50$  matrices whose entries were populated with standard normal distribution, demonstrated in Figure 6. As  $n$  increases, the histogram of eigenvalues becomes increasingly round.

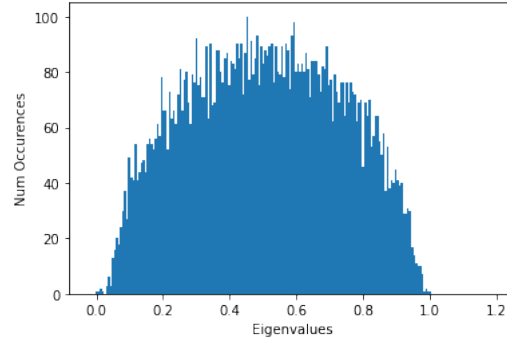


Figure 6: Histogram of eigenvalues from 200 RSN

For example, when the process is repeated for 5000 matrices, the histogram resembles a much smoother semi-circle (Figure 7). It was later discovered that the Wigner Semi-Circle shows no similarity to observed distribution in atomic spectra. However, it turns out to be a prominent distribution in graph and number theory: the Sato-Tate distribution[2]. This is an example about how curiosity within one branch of the Tree of Quantum Chaos, quantum physics, led to connections with the other branches, number theory and graph theory.

When the process of generating real, symmetric  $50 \times 50$  random matrices is done with uniform rather than normal distribution, the histogram of normalized eigenvalues bears no resemblance to a semi-circle. Figure 8 demonstrates this

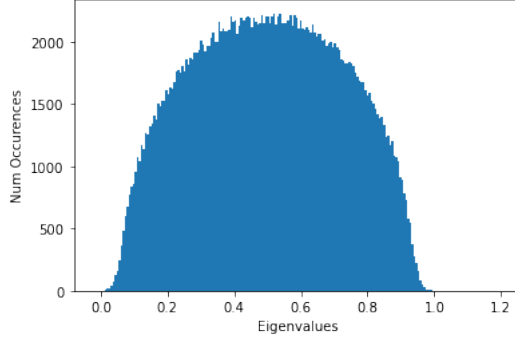


Figure 7: Histogram of eigenvalues from 5000 RSN

with 200 real, symmetric  $50 \times 50$  matrices chosen with uniform distribution. There is a curious shape here, however, with most eigenvalues clumping around  $\bar{\lambda} = 0.15258$ , and about 50 outliers near 1. Additionally, Table 4 indicates that the standard deviation  $\sigma$  for 200 real, symmetric  $50 \times 50$  matrices chosen with normal distribution is 0.23114, while  $\sigma$  for those chosen with uniform distribution is 0.13255. What this tells us is that in the case of 200 RSN, values are more distributed slightly further from the mean, while for 200 RSU the values tend to cluster closer to the mean.

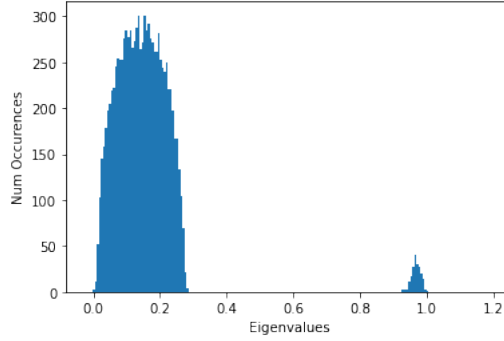


Figure 8: Histogram of eigenvalues from 200 RSU

### 4.3 Varying Success Rate for Random Adjacency Matrices

A pattern occurs when the success rate  $p$  of the binomial distribution used to populate random ‘adjacency’ matrices is varied. To recap,  $p$  is the probability that 1 is chosen out of choices 0 and 1. If  $p$  is increased, it is therefore more likely for a random ‘adjacency’ matrix to contain an increased amount of entries

populated with ‘1’. This directly corresponds to a graph with an increase of edges between vertices. Interestingly enough, the varying success rate has a dramatic impact on the eigenvalues of these matrices. As demonstrated in Table

Table 3: Statistics when  $p$  is Varied

	0.10	0.25	0.5	0.75	0.99
$\lambda$	0.40288	0.28940	0.19899	0.15884	0.05355
$\sigma$	0.22645	0.19127	0.15547	0.13809	0.13618
$\tilde{\sigma}$	0.24640	0.28449	0.33879	0.36804	0.46676
$\xi$	0.02039	0.01359	0.00887	0.00672	0.00353
$\tilde{\xi}$	0.29667	0.22926	0.14885	0.09621	0.02300

3, the average  $\bar{\lambda}$  of the normalized eigenvalues shifts closer to 0 as the success rate increases. Furthermore, the centralization  $\tilde{\sigma}$  increases, meaning that there is an increase in average distance from  $\frac{1}{2}$ , while the standard deviation  $\sigma$  decreases, indicating that the eigenvalues are in closer range to the mean  $\bar{\lambda}$ . These trends can also be seen visually. For example, notice how the spread of eigenvalues decreases as  $p$  increases from 0.25 (Figure 9) to 0.75 (Figure 10). Note that there is always one normalized eigenvalue at 1. This means pre-normalization, one eigenvalue is always much larger than the others.

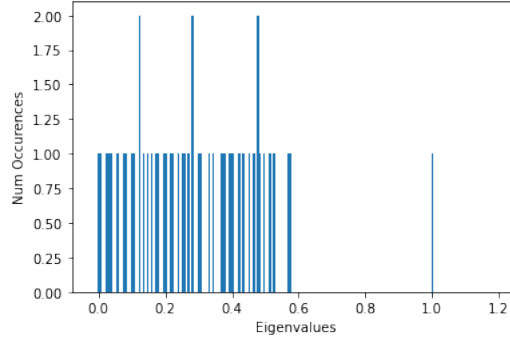


Figure 9: Eigenvalues of Random Adjacency Matrix,  $p = 0.25$

In addition to observing how the success rate impacts the spread of eigenvalues of  $50 \times 50$  random adjacency matrices, there is a noticeable visual similarity between a  $50 \times 50$  random adjacency matrix when  $p = 0.75$  and a single  $50 \times 50$  real symmetric matrix populated with uniform distribution. This is surprising given that the uniform distribution is symmetric around the mean; it would be intuitive for a single real symmetric matrix populated with uniform distribution to be similar to a random adjacency matrix with  $p = 0.5$ . This is because a success rate of 0.5 would yield a roughly even amount of 0’s and 1’s, becoming roughly symmetric about the mean. The similarity between a  $50 \times 50$  random

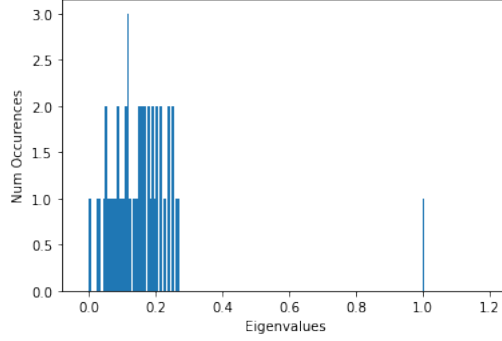


Figure 10: Eigenvalues of Random Adjacency Matrix,  $p = 0.75$

adjacency matrix when  $p = 0.75$  and a real, symmetric matrix populated uniformly can be viewed visually with Figure 10 and Figure 11. In both cases, eigenvalues are confined within the range of 0 to about 0.3, with 1 eigenvalue at 1. This is confirmed statistically: in the case of the real symmetric uniform matrix,  $\bar{\lambda}$  is 0.15443 and  $\sigma$  is 0.13956. In the case of the adjacency matrix where  $p = 0.75$ ,  $\bar{\lambda}$  is 0.15584 and  $\sigma$  is 0.13809.

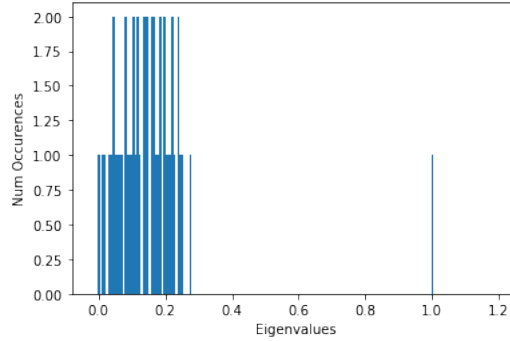


Figure 11: Eigenvalues for 50x50 Real, Symmetric, Uniform Matrix

#### 4.4 Poisson Spectrum and Applications

In “Finite Quantum Chaos”, Terras mentions the importance of the Poisson spectrum in arithmetic quantum chaos and quantum physics, two branches on the Tree of Quantum Chaos[3]. Arithmetic quantum chaos (the geometry of number theory) is outside the scope of this paper, but Terras makes an interesting note that Poisson level spacing may be a universal feature of arithmetic systems[2]. Additionally, in the vein of quantum physics, Terras notes that “it is currently believed that for all integrable systems, the eigenvalues follow the

Poisson behavior” [2]. The takeaway is that the Poisson spectrum provides a sort of universal model for both arithmetic quantum chaos and quantum physics, and that it may indicate a form of fundamental connection between them. There is also potential for the Poisson spectrum to draw connections between other roots and branches of the Quantum Chaos Tree. The mathematics behind these ideas is outside the scope of this paper. However, for the sake of its importance, the Poisson spectrum has been analyzed in the same manner as other cases.

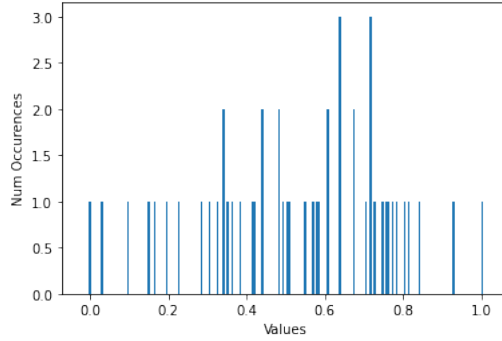


Figure 12: 50 Numbers from Poisson Spectrum

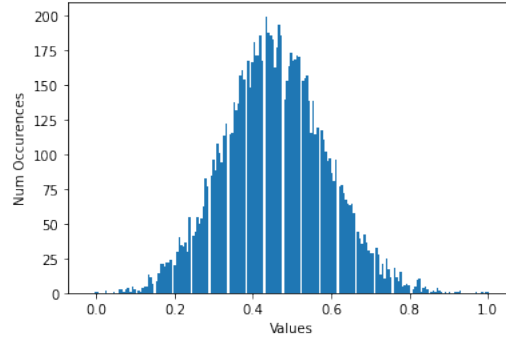


Figure 13: 10000 Numbers from Poisson Spectrum

With the Poisson distribution, numbers tend to occur more frequently near the specified time-interval variable. For the purpose of this paper, this was chosen as 500, but after normalizing the range of numbers to  $[0, 1]$ , values will be a fraction of the highest number sampled. The likelihood of a number being chosen decreases when the number is further from the time-interval variable, but it is still possible for a very large number to be chosen. This would considerably shift (to the left) the location of where the values cluster around in the normalized range. In contrast, if the largest number sampled is small, then this location will shift to the right. Note that in Figure 12, when 50 values are

selected from the Poisson spectrum, this indeed happens; the largest number chosen was smaller than usual, so when the values are normalized, they cluster slightly high near 0.65. However, when 10000 values are selected from the Poisson spectrum in Figure 13, the values appear to cluster just under 0.5. Thus, choosing more values makes outlying values less significant in their impact on the skew post-normalization. An interesting way to study this impact would be to calculate the probability distribution of each number being sampled as the largest number, when the time-interval variable is 500 and 10000 values are sampled. The discovery that random variables impact our normalization procedure grants us new ideas for normalization that will be discussed in Section 5.

The Poisson spectrum is not statistically similar to any eigenvalue distributions, which is demonstrated in Table 4. If integrable eigenvalue systems, as Terras states, are indeed supposed to look like the Poisson spectrum, then our eigenvalue distributions do not necessarily model atomic spectra. Molecules are very complicated and infinite-dimensional, and the graph models gathered in this paper are distinct from the Poisson distribution. However, while our eigenvalue systems do not necessarily model quantum physics, they have interesting structure in their own right. They may provide inspiration for discovering connections between different branches and roots on the Tree of Quantum Chaos (Figure 1), as well as insight into graph theory itself.

## 5 Future Work

Finding connections between all of the branches and roots of the Tree of Quantum Chaos (Figure 1) is a huge undertaking that many mathematicians have been working on. The potential knowledge to be discovered is immense. While this paper focused only on the relationship between two of the branches of the Tree, quantum physics and graphs, there is still much more that could be done between these two branches alone. For instance, many of the mathematical observations made in this paper could be further interpreted through the lens of quantum physics. It would also be interesting to model simple molecules as graphs, then calculate the eigenvalues of their adjacency matrices and compare them to the eigenvalues from the matrices from this paper, along with the uniform and Poisson spectra.

As discussed in Section 4.4, our normalization procedure is affected by random variables. In the future, we could create a different scaling system that is non-random, rather than using the smallest and largest numbers which, by its nature, has a random component to it for the probability distributions of random matrices and spectra. The current way we normalize spectra may make them difficult to analyze. In the future, we could use a fixed scaling system.

Other future work may include seeking the answer to the following question: what does it mean that the eigenvalues of a real, symmetric  $50 \times 50$  matrix populated uniformly looks more like the eigenvalues of a random adjacency matrix where  $p = 0.75$  than the eigenvalues of a random adjacency matrix

where  $p = 0.5$ ? Another idea is to observe more symmetry groups. In particular, investigating the hypothesis that creating adjacency matrices from star graphs would yield symmetrical eigenvalue spectra. Finally, future work could include seeking connections between graph theory, quantum physics, and other roots and branches of the Tree of Quantum Chaos.

## References

- [1] Pritha Bhandari. *The Standard Normal Distribution — Examples, Explanations, Uses*. 2020. URL: <https://cdn.scribbr.com/wp-content/uploads/2020/10/standard-normal-distribution-768x475.png>.
- [2] Audrey Terras. *Finite Models for Arithmetical Quantum Chaos*. Lecture Notes. URL: <https://mathweb.ucsd.edu/~aterras/newchaos.pdf>.
- [3] Audrey Terras. “Finite Quantum Chaos”. In: *The American Mathematical Monthly* 109.2 (2002), pp. 121–139. DOI: <https://doi.org/10.2307/2695325>.

## Acknowledgements

I would like to thank Dr. Joyce for mentoring me and for helping me see this year-long project through from beginning to end. I would also like to thank Dr. Amdeberhan for teaching Senior Seminar and making sure all of us seniors graduate with great math papers.

## Appendix

### Code Resources:

This GitHub Repository contains all the code necessary to reproduce my findings from this paper: <https://github.com/kromer-creator/Senior-Seminar-Research>.

### Tools:

- SageMath
- Python with Numpy and Matplotlib
- Jupyter Notebook